Modelling of Shear Zones in Granular Materials within Hypoplasticity

Jacek Tejchman

Civil Engineering Department, Gdansk University of Technology,
80-952 Gdansk, Poland
tejchmk@pg.gda.pl

Abstract. This paper presents a FE-analysis of shear localization in granular bodies with a finite element method based on a hypoplastic constitutive law. The law can reproduce essential features of granular bodies in dependence on the void ratio, pressure level and deformation direction. To simulate the formation of a spontaneous shear zone inside of cohesionless sand during plane strain compression, a hypoplastic law was extended by polar, non-local and gradient terms. The effects of 3 different models on the thickness of a shear zone was investigated.

1 Introduction

Localization of deformation in the form of narrow zones of intense shearing can develop in granular bodies during processes of granular flow or shift of objects with sharp edges against granular materials. Shear localization can occur spontaneously as a single zone, in several zones or in a regular pattern. They can also be induced in granular bodies along walls of stiff structures at granular bodies. An understanding of the mechanism of the formation of shear zones is important since they act as a precursor to ultimate failure.

Classical FE-analyses of shear zones are not able to describe properly both the thickness of localization zones and distance between them since they suffer from a spurious mesh sensitivity (to mesh size and alignment). The rate boundary value problem becomes ill-posed. (i.e. the governing differential equations of equilibrium or motion change the type by losing ellipticity for static and hiperbolicity for dynamic problems) [1]. Thus, the localization is reduced to a zero-volume zone. To overcome this drawback, classical constitutive models require an extension in the form of a characteristic length to regularize the rate boundary value problem and to take into account the microstructure of materials (e.g. size and spacing of micro-defects, grain size, fiber spacing). Different strategies can be used to include a characteristic length and to capture properly the post-peak regime (in quasi-static problems): polar models [2], non-local models [3] and gradient models [4].

In this paper, a spontaneous shear localization in granular bodies was investigated with a finite element method based on a hypoplastic constitutive law extended by polar, non-local and gradient terms.

M. Bubak et al. (Eds.): ICCS 2004, LNCS 3037, pp. 340–347, 2004.

2 Hypoplasticity

Hypoplastic constitutive models [5], [6] are an alternative to elasto-plastic ones for continuum modelling of granular materials. In contrast to elasto-plastic models, a decomposition of deformation components into elastic and plastic parts, yield surface, plastic potential, flow rule and hardening rule are not needed. The hypoplastic law includes barotropy (dependence on pressure level), pycnotropy (dependence on density), dependence on the direction of deformation rate, dilatancy and contractancy during shearing with constant pressure, increase and release of pressure during shearing with constant volume, and material softening during shearing of a dense material. The feature of the model is a simple formulation and procedure for determination of material parameters with standard laboratory experiments [7]. Owing to that one set of material parameters is valid within a large range of pressures and densities. The constitutive law can be summarised as follows:

$$\overset{o}{\sigma}_{ij} = f_s [L_{ij}(\hat{\sigma}_{kl}, d_{kl}) + f_d N_{ij}(\hat{\sigma}_{ij}) \sqrt{d_{kl} d_{kl}}] , \tag{1}$$

$$L_{ij} = a_1^2 d_{ij} + \hat{\sigma}_{ij} \hat{\sigma}_{kl} d_{kl} , \qquad N_{ij} = a_1 (\hat{\sigma}_{ij} + \hat{\sigma}_{ij}^{*}), \tag{2}$$

$$\overset{o}{\sigma}_{ij} = \overset{\bullet}{\sigma}_{ij} - w_{ik} \sigma_{kj} + \sigma_{ik} w_{kj} , \tag{3}$$

$$d_{ij} = 0.5 (v_{i,j} + v_{j,i}) , \qquad w_{ij} = 0.5 (v_{i,j} - v_{j,i}) , \tag{4}$$

$$\hat{\sigma}_{ij} = \frac{\sigma_{ij}}{\sigma_{kk}} , \qquad \hat{\sigma}_{ij}^{*} = \hat{\sigma}_{ij} - \frac{1}{3} \delta_{ij} , \tag{5}$$

$$f_s = \frac{h_s}{n h_i} \left(\frac{1 + e_i}{e} \right) \left(- \frac{\sigma_{kk}}{h_s} \right)^{1-n} , \qquad h_i = \frac{1}{c_1^2} + \frac{1}{3} - \left(\frac{e_{i0} - e_{d0}}{e_{c0} - e_{d0}} \right)^{\alpha} \frac{1}{c_1 \sqrt{3}} , \tag{6}$$

$$\overset{\bullet}{e} = (1 + e) d_{kk} , \qquad f_d = \left(\frac{e - e_d}{e_c - e_d} \right)^{\alpha} , \tag{7}$$

$$e_d = e_{d0} \exp[-(-\sigma_{kk} / h_s)^n], \qquad e_i = e_{i0} \exp[-(-\sigma_{kk} / h_s)^n], \tag{8}$$

$$e_c = e_{c0} \exp[-(-\sigma_{kk} / h_s)^n], \tag{9}$$

$$a_1^{-1} = c_1 + c_2 \sqrt{\hat{\sigma}_{kl}^{*} \hat{\sigma}_{lk}^{*}} \, [1 + \cos(3\theta)], \qquad \cos(3\theta) = - \frac{\sqrt{6}}{[\hat{\sigma}_{kl}^{*} \hat{\sigma}_{kl}^{*}]^{1.5}} (\hat{\sigma}_{kl}^{*} \hat{\sigma}_{lm}^{*} \hat{\sigma}_{mk}^{*}), \tag{10}$$

$$c_1 = \sqrt{\frac{3}{8}} \frac{(3 - \sin\phi_c)}{\sin\phi_c} , \qquad c_2 = \frac{3}{8} \frac{(3 + \sin\phi_c)}{\sin\phi_c} , \tag{11}$$

wherein: σ_{ij} - Cauchy stress tensor, e – current void ratio, $\overset{o}{\sigma}_{ij}$ - Jaumann stress rate tensor, $\hat{\sigma}_{ij}$ - normalised stress tensor, $\hat{\sigma}_{ij}^{*}$ - deviatoric part of the normalised stress tensor, d_{ij} - rate of deformation tensor, w_{ij} - spin tensor, $v_{i,j}$ - gradient of velocity, f_s -

stiffness factor, f_d – density factor, h_s - granular hardness, θ - Lode angle, e_c - critical void ratio, e_d – minimum void ratio, e_i - maximum void ratio, e_{i0} - maximum void ratio at pressure equal to zero, e_{d0} - minimum void ratio at pressure equal to zero, e_{c0} - critical void ratio at pressure equal to zero, ϕ_c - critical angle of internal friction during stationary flow, n – compression coefficient, α - pycnotropy coefficient, a_1 – coefficient determining the shape of the stationary stress surface.

The constitutive relationship requires 7 material constants: e_{i0}, e_{d0}, e_{c0}, ϕ_c, h_s, n and α. The FE-analyses were carried out with the following material constants (for so-called Karlsruhe sand): e_{i0}=1.3, e_{d0}=0.51, e_{c0}=0.82, ϕ_c=30°, h_s=190 MPa, n=0.5 and α=0.3 [6].

A hypoplastic constitutive law cannot describe realistically shear localization since it does not include a characteristic length. A characteristic length was taken into account by means of a polar, non-local and gradient theory.

3 Enhanced Hypoplasticity

3.1 Polar Hypoplasticity

The polar terms were introduced in a hypoplastic law (Eqs.1-11) with the aid of a polar (Cosserat) continuum [2]. Each material point has for the case of plane strain three degrees of freedom: two translational degrees of freedom and one independent rotational degree of freedom. The gradients of the rotation are connected to curvatures which are associated with couple stresses. It leads to a non-symmetry of the stress tensor and a presence of a characteristic length.

The constitutive law can be summarised for plane strain as follows [9], [10] (Eqs.3-11 and Eqs.12-17):

$$\overset{o}{\sigma}_{ij} = f_s [L_{ij}(\hat{\sigma}_{kl}, \hat{m}_k, d^c_{kl}, k_k d_{50}) + f_d N_{ij}(\hat{\sigma}_{ij}) \sqrt{d^c_{kl} d^c_{kl} + k_k k_k d^2_{50}}] , \tag{12}$$

$$\overset{o}{m}_i / d_{50} = f_s [L^c_i(\hat{\sigma}_{kl}, \hat{m}_k, d^c_{kl}, k_k d_{50}) + f_d N^c_i(\hat{m}_i) \sqrt{d^c_{kl} d^c_{kl} + k_k k_k d^2_{50}}] , \tag{13}$$

$$L_{ij} = a_1^2 d^c_{ij} + \hat{\sigma}_{ij}(\hat{\sigma}_{kl} d^c_{kl} + \hat{m}_k k_k d_{50}), \quad L^c_i = a_1^2 k_i d_{50} + a_1^2 \hat{m}_i(\hat{\sigma}_{kl} d^c_{kl} + \hat{m}_k k_k d_{50}), \tag{14}$$

$$N_{ij} = a_1(\hat{\sigma}_{ij} + \hat{\sigma}^*_{ij}), \qquad N^c_i = a_1^2 a_c \hat{m}_i , \tag{15}$$

$$\overset{o}{m}_i = \overset{\bullet}{m}_i - 0.5 w_{ik} m_k + 0.5 m_k w_{ki} , \tag{16}$$

$$d^c_{ij} = d_{ij} + w_{ij} - w^c_{ij}, \qquad k_i = w^c_{,i}, \qquad w_{kk} = 0, \qquad w_{21} = -w_{12} = w^c , \tag{17}$$

wherein m_i – Cauchy couple stress vector, $\overset{o}{m}_i$ – Jaumann couple stress rate vector, d^c_{ij} – polar rate of deformation tensor, k_i – rate of curvature vector, w^c – rate of Cosserat rotation, d_{50} – mean grain diameter, a_c – micro-polar constant (a_c=a_1^{-1}) [10].

3.2 Nonlocal Hypoplasticity

A non-local approach is based on spatial averaging of tensor or scalar state variables in a certain neighbourhood of a given point (i.e. material response at a point depends both on the state of its neighbourhood and the state of the point itself). To obtain a regularisation effect for both the mesh size and mesh inclination, it is sufficient to treat non-locally only one internal constitutive variable (e.g. equivalent plastic strain in an elasto-plastic formulation [4] or measure of the deformation rate in a hypoplastic approach [11]) whereas the others can retain their local definitions. In the hypoplastic calculations, the non-local measure of the deformation rate $d = \sqrt{d_{kl} d_{kl}}$ in Eq.1 was treated non-locally:

$$d^*(x) = \frac{1}{A} \int_{-\infty}^{\infty} w(r)\, d(x+r) dV \,, \qquad w(r) = \frac{1}{l\sqrt{\pi}} e^{-(\frac{r}{l})^2} \,, \tag{18}$$

where r is the distance from the material point considered to other integration points of the entire material body, w is the weighting function (error density function) and A is the weighted volume. The parameter l denotes a characteristic length (it determines the size of the neighbourhood influencing the state at a given point).

3.3 Gradient Hypoplasticity

The gradient approach is based on the introduction of a characteristic length by incorporating higher order gradients of strain or state variables into the constitutive law [4]. By expanding e.g. the non-local measure of the deformation rate $d(x+r)$ in Eq.18 into a Taylor series around the point r=0, choosing the error function w as the weighting function (Eq.19), cancelling odd derivative terms and neglecting the terms higher than the second order one can obtain the following expression (2D-problems):

$$d^*(x,y) = d + \frac{l^2}{4}\left(\frac{\partial^2 d}{\partial x^2} + \frac{\partial^2 d}{\partial y^2} + 2\frac{\partial^2 d}{\partial x \partial y}\right), \tag{19}$$

where l is a characteristic length. To evaluate the gradient term of the measure of the deformation rate d and to consider the effect of adjacent elements, a standard central difference scheme was used [12]:

$$(\nabla^2)^I d = \sum_n \left(\frac{\Delta^2}{\Delta x_n^2}\right)^I d = \sum_n \frac{\dfrac{d^{I+1} - d^I}{x_n^{I+1} - x_n^I} - \dfrac{d^I - d^{I-1}}{x_n^I - x_n^{I-1}}}{x_n^{i+1} - x_n^i} \,, \qquad n = x, y, z \,, \tag{20}$$

where "i" denotes a grid point and "I" a grid element.

4 FE-Results

The FE-calculations of plane strain compression tests were performed with a sand specimen which was h_o=10 cm high and b=2 cm wide (length l=1.0 m). As the initial stress state, the state with $\sigma_{22}=\sigma_c+\gamma_d x_2$ and $\sigma_{11}=\sigma_c$ was assumed in the sand specimen where σ_c denotes the confining pressure (σ_c=0.2 MPa), x_2 is the vertical coordinate measured from the top of the specimen, γ_d denotes the initial volume weight (σ_{11} - horizontal normal stress, σ_{22} - vertical normal stress).

A quasi-static deformation in sand was initiated through a constant vertical displacement increment prescribed at nodes along the upper edge of the specimen.. To preserve the stability of the specimen against the sliding along the bottom boundary, the node in the middle of the bottom was kept fixed.

To numerically obtain a shear zone inside of the specimen, a weaker element with a higher initial void ratio, e_0=0.90, was inserted in the middle of the left side.

4.1 Polar Hypoplasticity

Figs.1 and 2 present the results of plane strain compression within polar continuum compared t. The normalized load-displacement curves with a different mean grain diameter (d_{50}=0 mm, 0.5 mm and 1.0 mm) in dense specimen (e_o=0.60, σ_c=0.2 MPa) are depicted in Fig.1. Fig.2 shows the deformed FE-meshes with the distribution of void ratio (the darker the region, the higher the void ratio).

The FE-results demonstrate that the larger the mean grain diameter, the higher the maximum vertical force on the top. The lower mean grain diameter, the larger the material softening (the behaviour of the material is more brittle). At the beginning, two shear zones are created expanding outward from the weakest element. Afterwards, and up to the end, only one shear zone dominates. The complete shear zone is already noticeable shortly after the peak. It is characterised both by a concentration of shear deformation and Cosserat rotation, and an increase of the void ratio. The thickness is about $t_{sz}\cong$6 mm=12$\times d_{50}$ (d_{50}=0.5 mm) and $t_{sz}\cong$10 mm=10$\times d_{50}$ (d_{50}=1.0 mm). An increase of the thickness of the shear zone with increasing d_{50} corresponds to a decrease of the rate of softening. The material becomes softer, and thus a larger deformation can develop. The calculated thickness of the shear zone in Karlsruhe sand (d_{50}=0.5 mm) is in accordance with experiments: $t_{sz}=13\times d_{50}$ [13] and $9\times d_{50}$ [14].

4.2 Nonlocal Hypoplasticity

The results with a non-local measure of the deformation rate d^* using a different characteristic length l of Eq.18 (l=0 mm, 0.5 mm, 1.0 mm and 2.0 mm) for dense sand (e_o=0.60, σ_c=0.2 MPa) are shown in Fig.3.

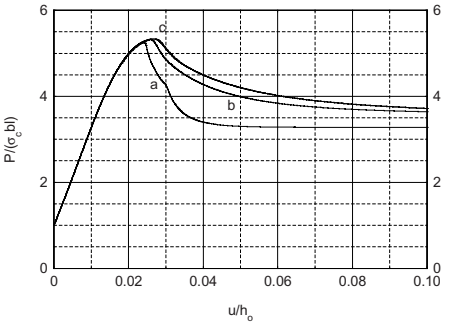

Fig. 1. Load-displacement curves (polar continuum): a) d_{50}=0.0 mm, b) d_{50}=0.5 mm, c) d_{50}=1.0 mm

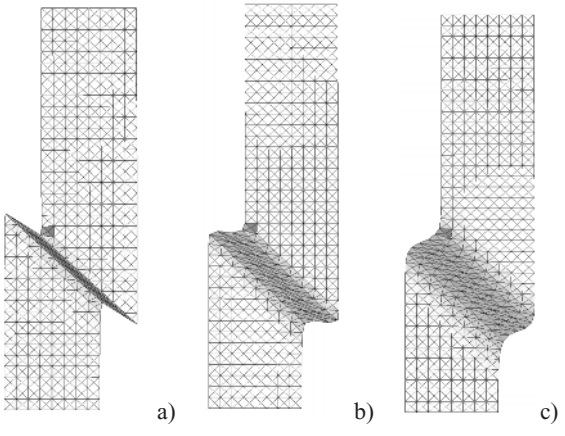

Fig. 2. Deformed FE-meshes with the distribution of void ratio in the residual state (polar continuum): a) d_{50}=0.0 mm, b) d_{50}=0.5 mm, c) d_{50}=1.0 mm

Similarly as in a polar continuum, the larger the characteristic length, the larger the maximum vertical force on the top and the smaller the material softening (the behaviour is more ductile). The vertical forces are almost the same as within a polar continuum. If the characteristic length is larger (l=2.0 mm), the shear zone does not appear. The thickness of the shear zone t_{sz} with l=0.5 mm is smaller than this with d_{50}=0.5 mm within a polar continuum. However, the thickness of the shear zone with l=1 mm is close to that within a polar continuum: $t_{sz} \cong 7$ mm=14×l=14×d_{50}. In general, the relationship between the non-local and polar characteristic length is $l \cong 2 \times d_{50}$ on the basis of the shear zone thickness.

4.3 Gradient Hypoplasticity

The results with a gradient measure of the deformation rate for dense sand (e_o=0.60, σ_c=0.2 MPa) are shown in Fig.4.

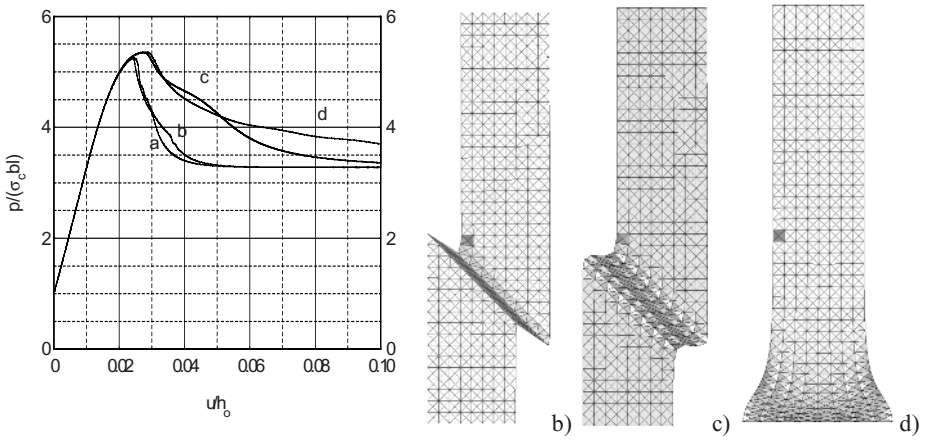

Fig. 3. Load-displacement curves and deformed FE-meshes with the distribution of void ratio in the residual state (non-local continuum): a) l=0 mm, b) l=0.5 mm, c) l=1.0 mm, d) l=2 mm

The evolution of the vertical force on the top is qualitatively similar as in the polar and non-local continuum. The thickness of the shear zone $t_{sz}\cong 7.3$ mm$\cong 7\times l$ (l=1.0 mm) is slightly larger than within a non-local continuum (l=1.0 mm) and a polar continuum (d_{50}=0.5 mm).

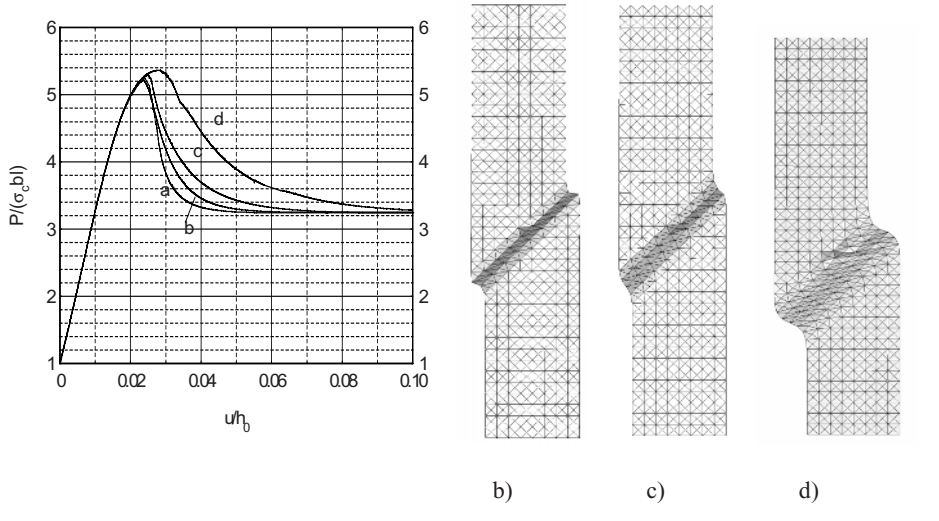

Fig. 4. Load-displacement curve and deformed FE-mesh with the distribution of void ratio in the residual state (gradient continuum): a) l=0 mm, b) l=0.5 mm, c) l=1 mm, d) l=2 mm

5 Conclusions

The results with a conventional hypoplastic constitutive model suffer from a mesh-dependency. The thickness of shear zones is severely mesh-dependent.

A polar, non-local and gradient hypoplastic model provide a full regularisation of the boundary value problem during plane strain compression. Numerical solutions converge to a finite size of the localization zone upon mesh refinement.

The thickness of the localized shear zone and the bearing capacity of the granular specimen increase with increasing characteristic length.

The characteristic length within a non-local and gradient theory can be related to the mean grain diameter on the basis of a basis of a back analysis of experiments.

References

1. de Borst, R., Mühlhaus, H.-B., Pamin, J., Sluys, L.: Computational modelling of localization of deformation. In: D. R. J. Owen, H. Onate, E. Hinton, editors, Proc. of the 3rd Int. Conf. Comp. Plasticity, Swansea, Pineridge Press (1992) 483-508
2. Tejchman, J., Wu, W.: Numerical study on shear band patterning in a Cosserat continuum. Acta Mechanica 99 (1993) 61-74
3. Bazant, Z., Lin, F., Pijaudier-Cabot, G.: Yield limit degradation: non-local continuum model with local strain, Proc. Int. Conf. Computational Plasticity, Barcelona. In: Owen, editor, (1987) 1757-1780
4. Zbib, H. M., Aifantis, E. C.: On the localisation and postlocalisation behaviour of plastic deformation. Res Mechanica 23 (1988) 261-277
5. Gudehus, G.: Comprehensive equation of state of granular materials. Soils and Foundations 36, 1 (1996) 1-12
6. Bauer, E.: Calibration of a comprehensive hypoplastic model for granular materials. Soils and Foundations 36, 1 (1996) 13-26
7. Herle, I., Gudehus, G.: Determination of parameters of a hypoplastic constitutive model from properties of grain assemblies, Mechanics of Cohesive-Frictional Materials 4, 5 (1999) 461-486
8. Oda, M.: Micro-fabric and couple stress in shear bands of granular materials. Powders and Grains. In: C. Thornton, editor, Rotterdam, Balkema (1993) 161-167.
9. Tejchman, J., Herle, I., Wehr, J.: FE-studies on the influence of initial void ratio, pressure level and mean grain diameter on shear localisation. Int. J. Num. Anal. Meth. Geomech. 23 (1999) 2045-2074
10. Tejchman, J.: Patterns of shear zones in granular materials within a polar hypoplastic continuum. Acta Mechanica 155, 1-2 (2002) 71-95
11. Tejchman, J.: Comparative FE-studies of shear localizations in granular bodies within a polar and non-local hypoplasticity. Mechanics Research Communications 2004 (in print)
12. Alehossein, H., Korinets, A.: Gradient dependent plasticity and the finite difference method. Bifurcation and Localisation Theory in Geomechanics. In: H.-B. Mühlhaus et all, editors, (2001) 117-125
13. Vardoulakis, I.: Scherfugenbildung in Sandkörpern als Verzweigungsproblem. Dissertation, Institute for Soil and Rock Mechanics, University of Karlsruhe 70 (1977).
14. Yoshida, Y., Tatsuoka, T., Siddiquee, M.: Shear banding in sands observed in plane strain compression. Localisation and Bifurcation Theory for Soils and Rocks, eds.: R. Chambon, J. Desrues and I. Vardoulakis, Balkema, Rotterdam (1994) 165-181